Dalton Transactions

Solid state characterization of oxidized actinides co-crystallized with uranyl nitrate hexahydrate

Journal:	*Dalton Transactions*
Manuscript ID	DT-COM-10-2019-004000.R1
Article Type:	Communication
Date Submitted by the Author:	15-Nov-2019
Complete List of Authors:	Einkauf, Jeffrey; Texas A&M University College Station, Center for Nuclear Security Science and Policy Initiatives Burns, Jonathan; Texas A&M University College Station, Nuclear Engineering and Science Center

COMMUNICATION

Solid state characterization of oxidized actinides co-crystallized with uranyl nitrate hexahydrate

Jeffrey D. Einkauf[a] and Jonathan D. Burns*[b]

Received 00th January 20xx,
Accepted 00th January 20xx

DOI: 10.1039/x0xx00000x

Characterization of the penta- and hexavalent dioxo cations of NpO_2^+, NpO_2^{2+}, PuO_2^{2+}, and AmO_2^{2+} has been carried out by diffuse reflectance UV-Vis-NIR spectroscopy, with the first observations of NpO_2^+, NpO_2^{2+}, and AmO_2^{2+} in the solid state. Absorbance measurements confirmed the presence of the higher actinides of Np, Pu, and Am, with shifts in their absorbance bands indicating the formation of the dinitrate species in the crystalline phase. The oxidized actinides were prepared in the solid state by co-crystallization with $UO_2(NO_3)_2{\cdot}6H_2O$ by a simple reduction in temperature. The hexavalent species were all co-crystallized in near proportion UO_2^{2+}, the pentavalent species was co-crystallized at in a slightly less efficient maner, roughly 83% to that of U(VI).

In this paper, we present solid-state analysis of highly oxidized actinides (An) co-crystallized in a uranyl nitrate hexahydrate (UNH) crystalline phase, which includes the first observed NpO_2^+, NpO_2^{2+}, and AmO_2^{2+} diffuse reflectance (DR) UV-Vis-NIR absorption spectra. This co-crystallization is a potentially transformational concept for actinide separations supporting a future sustainable nuclear fuel cycle by co-crystallization of actinyl nitrate salts. The increasing emission of greenhouse gases worldwide makes urgent the need to accelerate development of sustainable nuclear fuel cycles as part of an overall solution to CO_2-free power supply.[1–3] Among the long-term problems that must be solved is an efficient separation of actinides from used nuclear fuel for the purposes of maximum energy utilization of the fuel and minimization of waste going to geologic storage, while serving the needs of nonproliferation.[1–3] Whereas separation and recycle of U and Pu provide the key to energy utilization, separation and recycle of the minor actinides (MAs i.e., Np and Am) are also necessary to minimize the heat load and long-term hazard of geologic storage.[4–8] While often included in the MAs, Cm has less significant long-term geological impact, due to the short half-life of the isotope produced during power generation. Additionally, its chemistry is less diverse compared to either Np or Am, as it does not form the actinyl dioxo cation. The best current technology practiced today involves the use of solvent extraction for the separation of U and Pu[9] but does not have the capability to remove and recycle the MAs, a deficiency that has stimulated considerable international research efforts over the past several decades.[10] Although new solvent-extraction methodology is emerging for this purpose, a major deterrent is the added cost of a separate MA separation.[11] A transformational solution overall may therefore entail group separation of actinides with a single technology, an idea that is under investigation in several laboratories around the world, primarily using complex solvent extraction approaches.[12,13] With the advent of methods to access the difficult AmO_2^{2+} oxidation state in nitric acid,[14,15] it may be possible to perform such a group separation of U to Am, but the instability of AmO_2^{2+} in the presence of the organic compounds raises questions about the feasibility of a group actinyl separation using solvent extraction. It was our thought that a simple and elegant solution would be to co-crystallize actinyl ions as their nitrate salts from nitric acid, which avoids the unwanted effects of organic reductants and could in principle accomplish an unprecedented group separation. In this work, we present spectroscopic characterization of the crystalline phase resulting from actinyl co-crystallization, with the first observed NpO_2^+, NpO_2^{2+}, and AmO_2^{2+} solid state absorbance spectra, a step towards confirming the previous proof-of-principle of our concept.[16,17]

As mentioned, we have recently proposed and demonstrated a hexavalent actinide co-crystallization separation, directly inspired by the group actinide extraction (GANEX)-type separation concept, where U through Am could be separated as crystalline nitrate salts.[16] The hexavalent actinides were removed from solution in near proportion to one another as UNH crystallized out of solution, while the lower valent species, like Pu^{4+} and Am^{3+}, were only slightly removed

[a] Center for Nuclear Security Science & Policy Initiatives, Texas A&M University, College Station, TX 77843, USA.
[b] Nuclear Engineering and Science Center, Texas A&M University, College Station, TX 77843, USA.
†Electronic Supplementary Information (ESI) available: [details of any supplementary information available should be included here]. See DOI: 10.1039/x0xx00000x

from solution. Later, a thorough investigation of the yield and selectivity of the AnO_2^{2+} co-crystallization into UNH showed yields of 80–90% recovery of the AnO_2^{2+} species could be expected with separation factor ≥81 from fission products like Cs^+, Sr^{2+}, Ln^{3+}, and Zr^{4+}.[17] Both studies were limited in that the crystalline phase was not investigated directly by chemical analysis, with only gamma (γ) spectroscopy, leaving the oxidation state of the minor constituents to be inferred by the solution speciation. In the case of AmO_2^{2+}, an increase in stability was observed by dissolving the AmO_2^{2+} containing UNH crystalline phase, which revealed a majority of the Am persisting as AmO_2^{2+} for at least 13 d within the crystalline phase (<3% reduced to Am^{3+}), while in solution over 50% reduced to Am^{3+} after only 10 d.[16]

An investigation was initiated to directly determine the oxidation state of the minor species, NpO_2^{2+}, PuO_2^{2+}, and AmO_2^{2+}, incorporated in the crystalline phase and to understand their coordination within the lattice. To accomplish this, several samples were produced by generating solutions with either NpO_2^{2+}, PuO_2^{2+}, or AmO_2^{2+} present by use of $NaBiO_3$ as a chemical oxidant. For the NpO_2^{2+} containing sample, a system containing concentrations of roughly 2.3 M UO_2^{2+} and 170 mM NpO_2^{2+} at a HNO_3 concentration of 1.4 M, was cooled from 52 ºC down to 25 ºC. As a result of cooling, an approximately near proportion removal of both UO_2^{2+} and NpO_2^{2+} was observed, with 96 ± 10% and 90 ± 6% crystallizing out from solution as UNH, respectively. Similarly, the PuO_2^{2+} containing sample was generated from a system containing concentrations of roughly 2.2 M UO_2^{2+} and 110 mM PuO_2^{2+} at a HNO_3 concentration of 6.6 M and resulted in a crystalline UNH product, again, with near proportion removal of the hexavalent An species, 86 ± 9% for UO_2^{2+} and 78 ± 5% for PuO_2^{2+}. Unlike NpO_2^{2+} or PuO_2^{2+}, AmO_2^{2+} is much more unstable, having Am(VI)/Am(III) reduction potentials on the order of +1.7 V vs NHE[14,18], requiring excess Bi(V) to be present in solution as holding oxidant. For this sample a system containing concentrations of roughly 2.8 M UO_2^{2+} and 42 mM AmO_2^{2+} in 2.8 M HNO_3 was left to naturally cool to room temperature. The resulting crystalline UNH product, with 79 ± 8% for UO_2^{2+} and 79 ± 6% for AmO_2^{2+} removed from solution, a near proportion removal of the AnO_2^{2+} species was observed. In addition to the hexavalent species, a sample containing NpO_2^+ was generated from a solution containing concentrations of roughly 3.1 M UO_2^{2+} and 150 mM NpO_2^+ at a HNO_3 concentration of 4.7 mM. While a near proportion removal from solution was not observed, NpO_2^+ was still removed at relatively large amount compared to UO_2^{2+}, 75 ± 5% and 90 ± 8%, respectively. This is not surprising, as the linear dioxo confirmation of actinyl cation is still present for NpO_2^+, the overall charge of the molecular ion is just reduced from 2+ down to 1+. The lower charge will result in a charge defect in the crystalline lattice wherever the NpO_2^+ is substituted, which will reduce the overall efficiency of the substitution. Table 1 summarizes the removal of the different actinyl species from solution. The uniform distribution of U and TRUs in the crystalline phases (*cf.* Fig. S1) was determined SEM-EDS measurements (*cf.* Fig. S8, Fig. S9, Fig. S10, and Fig. S11).

Once the crystalline phases had been generated, determination of the speciation of the An species was carried out. To do this, DR UV-Vis-NIR spectroscopy was employed. As can be seen in Fig. 1, both the solution absorption spectra of the uranyl nitrate crystallization solution and the Kubelka-Munk function of pure UNH crystals have very similar spectra, with only a slight shift the maximum absorbance at 415 nm to 418 nm, along with the relative intensity of the satellite bands to favor the higher wavelength features over those at lower wavelengths.

Table 1: Recrystallization yields and ratios of the percent crystallization of different TRU species with respect to UO_2^{2+} in UNH

TRU Species	% Crystallized U	% Crystallized TRU	Ratio U:TRU
Blank	89% ± 9%	-	
NpO_2^{2+}	96% ± 10%	90% ± 6%	1.1
PuO_2^{2+}	86% ± 9%	78% ± 5%	1.1
AmO_2^{2+}	79% ± 8%	79% ± 6%	1.0
NpO_2^+	90% ± 9%	75% ± 5%	1.2

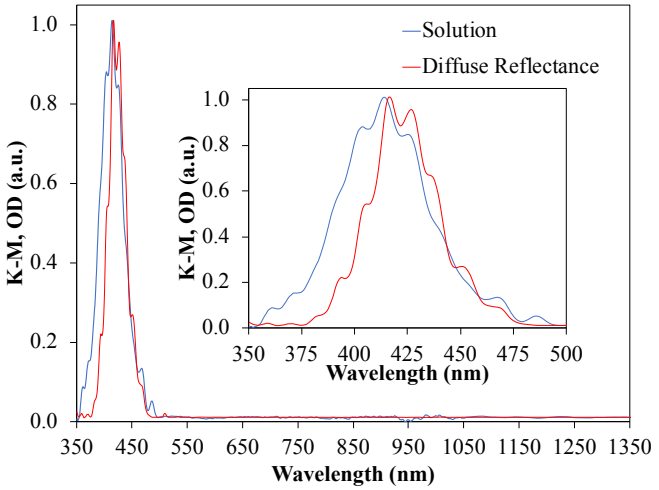

Fig. 1 Absorbance spectra of the uranyl nitrate solution prior to crystallization diluted 50-fold (blue) and Kubelka-Munk function of the crystallized UNH (red) normalized to 1 for comparison. Inset shows zoomed in region from 350–500 nm.

Alternatively, the NpO_2^{2+} absorbance is affected significantly by being incorporated into the UNH crystal lattice (*cf.* Fig. 2). The most obvious change is in the primary absorbance at 1222 nm, which undergoes a hypsochromic shift to 1089 nm and reduces significantly in relative intensity. The NpO_2^{2+} band at 1089 nm has not previously been directly observed in the dinitrate system; however, Lindqvist-Reis *et al.* reported a transition at 1080 nm revealed through peak deconvolution, which was attributed to two trans nitrate ions coordinated in a bidentate fashion to the neptunyl ion.[19] The diminished intensity of the 1089 nm band in the crystalline phase is believed to be a result of high symmetry, which is completely absent in other high symmetry systems.[20] The absorbance band at 556 nm that typically are the defining feature for NpO_2^{2+} in the solid-state[20] appears to remain relatively unchanged, with only a negligible shift up to 558 nm. Several bands in the crystalline phase can be clearly observed, which are not visible in the solution at 513 nm, 595 nm, 614 nm, 621 nm, and

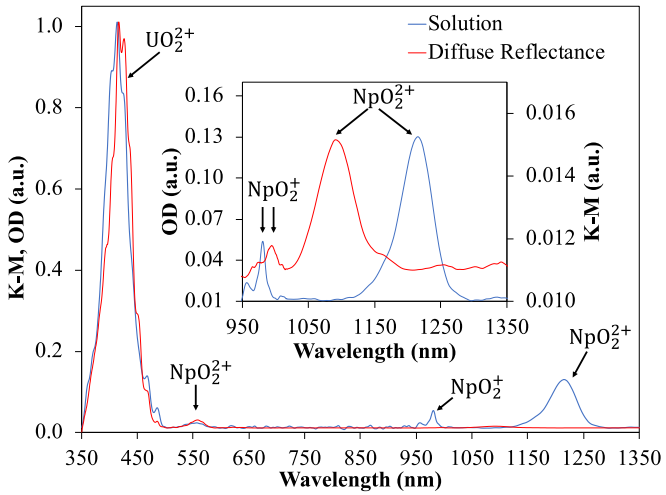

Fig. 2 Absorbance spectra of the NpO_2^{2+} uranyl nitrate solution prior to crystallization diluted 115-fold (blue) and Kubelka-Munk function of the crystallized UNH with NpO_2^{2+} incorporated (red) normalized to 1 for comparison. Inset shows zoomed in region from 950–1350 nm (it should be noted, the K-M is magnified 10-fold relative the OD).

636 nm, arising from the vibronic coupling for NpO_2^{2+}, which are believed to be a result, in part, of increasing the concentration of the Np ion per volume upon crystallization.[20] Lastly, and as will be discussed in detail below, the absorbance from residual NpO_2^{+} at 981 nm shifts to 994 nm.

As with the NpO_2^{2+}, the PuO_2^{2+} absorbance is affected significantly by being incorporated into the UNH crystal lattice (*cf.* Fig. 3). The most obvious change is in the primary absorbance at 830 nm, which reduces in relative intensity, broadens considerably, and splits, shifting down to 801 nm and 812 nm upon coordination of the two nitrate ions, which are in line with what Gaunt *et al*. previously observed.[21] In the crystalline phase, there are several additional observable PuO_2^{2+} bands in the NIR region at 920 nm, 933 nm, 977 nm, 983 nm, 1001 nm, 1147 nm, and 1227 nm; while the solution phase only has 953 nm, 983 nm, and 1075 nm. There are also a number of differences in the visible range of the crystalline phase to that of the solution. To begin with, the feature in the range of 510–585 nm has a more distinct fine structure, with distinct transition at 527 nm, 537 nm, and 556 nm previously assigned as transitions in the $^3H_{4g} \rightarrow {}^3\Pi_{2g}$ region.[21] Other noticeable changes are in the range of 600–700 nm, where the sharp absorbance at 624 nm and the broad, convoluted absorbance at 660 nm of the solution phase are replaced with weak, broad absorbances at 628 nm and 674 nm in the crystalline phase.

Next the crystalline phase with AmO_2^{2+} incorporated was examined. At first glance, Am containing spectra appear more difficult to interpret, with all three of the stable oxidation states Am^{3+} (10%), AmO_2^{+} (12%), and AmO_2^{2+} (78%) present in both the solution and crystalline phase, as shown in Fig. 4. However, many of the absorbance bands for all three oxidation states remain completely unaltered in the crystalline phase compared to the solution phase. In addition to these unchanged bands, there are several changes in the spectrum of the crystalline phase, specifically the appearance of a band at 995 nm. This new band is believed to originate from AmO_2^{2+} incorporated into the UNH lattice in the place of UO_2^{2+}, while the unaltered

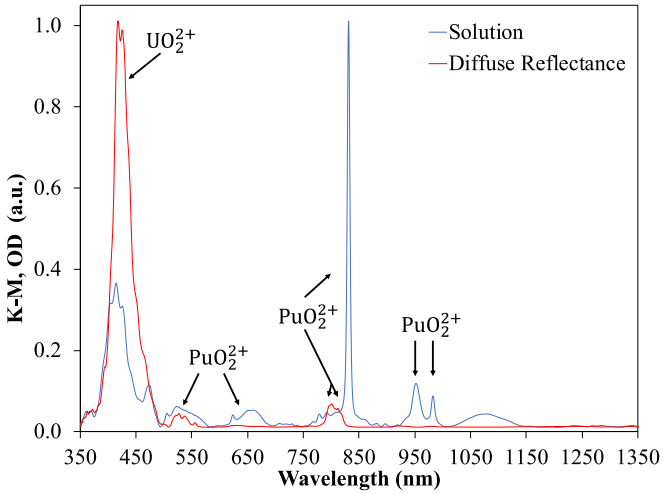

Fig. 3 Absorbance spectra of the PuO_2^{2+} uranyl nitrate solution prior to crystallization diluted 100-fold (blue) and Kubelka-Munk function of the crystallized UNH with PuO_2^{2+} incorporated (red) normalized to 1 for comparison.

bands arise from Am adhered to the surface due to an incomplete phase separation of the solution and crystalline phases. At this point it should be noted, in attempt to prevent excess reduction of the Am(VI) to Am(III) with organic species from the cellulose acetate filter or plastic housing of the tube filter, the phases were separated by decantation rather than centrifugation. To determine if the unchanged Am(III), Am(V), and Am(VI) were indeed from surface adherence of the mother liquor on the crystals, a DR spectrum was obtained again after 8 d (10 after crystallization), sufficient time for the Am(VI) to begin to reduce. As can be seen in Fig. 5, the Am(VI) absorbance at 996 nm was completely removed, while the Am(III) absorbances increased by roughly 10% relative to the UO_2^{2+} absorbance, indicating reduction had occurred. Upon washing a portion of the crystalline phase with a solution of cold *ca.* 1.9 M UO_2^{2+} and acidity of 8 M HNO_3, the Am^{3+} absorbance diminished

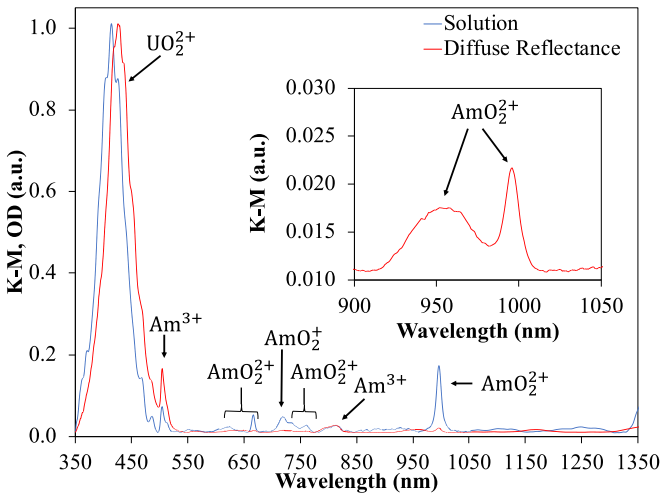

Fig. 4 Absorbance spectra of the AmO_2^{2+} uranyl nitrate solution prior to crystallization diluted 39-fold (blue) and Kubelka-Munk function two days after crystallization of the UNH with AmO_2^{2+} incorporated (red) normalized to 1 for comparison. Inset shows zoomed in region from 900–1050 nm. It should be noted,

all three of the stable oxidation states Am^{3+} (10%), AmO_2^+ (12%), and AmO_2^{2+} (78%) present in both the solution and crystalline phase.

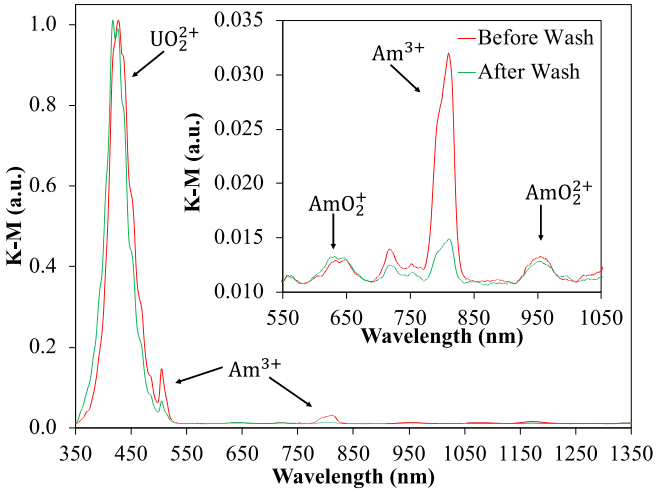

Fig. 5 Kubelka-Munk function 10 d after crystallization of the UNH with AmO_2^{2+} incorporated before washing (red), and after washing a portion of the crystals with 20 µL of cold *ca.* 1.9 M UO_2^{2+} and acidity of 8 M HNO_3 (green) normalized to 1 for comparison. Inset shows zoomed in region from 550–1050 nm.

significantly, decreasing over 70% relative to the UO_2^{2+} absorbance, while the band of the AmO_2^{2+} incorporated into the UNH lattice remained relatively constant. Another indication that surface adhesion of the mother liquor to the crystalline phase had occurred is by examining UO_2^{2+} absorbance; prior to washing, the UO_2^{2+} absorbance, while still shifted, has a very similar structure to that in solution. After washing, the structure of the UO_2^{2+} absorbance is similar to the other crystalline phases discussed earlier.

Lastly, the absorbance spectrum of NpO_2^+ was also impacted by being incorporated into the crystalline phase (*cf.* Fig 6). As mentioned earlier, the most distinct change is that of the NpO_2^+ primary absorbance at 981 nm, which shifted to 994 nm. The satellite band at 1024 nm in solution becomes less pronounced in the crystalline phase, transforming into a shoulder of the 994 nm band. The band at 1094 nm reduces in relative intensity and broadens, while a new absorbance band at 1162 nm appears. Last the absorbance at 617 nm also reduces in relative intensity upon NpO_2^+ being incorporated into the crystalline phase. The reason behind the bathochromic shift of the transition at 981 nm to 994 nm, and not to a lower wavelength like previous observed in the other AnO_2^{2+} samples, upon crystallization is currently under investigation.

Conclusions

In conclusion, during the search for a simplified method of actinide separation for economical nuclear fuel recycle, the first observed solid state absorbance spectra of NpO_2^+, NpO_2^{2+}, and AmO_2^{2+} have been obtained. Each of the hexavalent TRU elements, NpO_2^{2+}, PuO_2^{2+}, and AmO_2^{2+}, have been co-crystallized with U(VI) out of nitric acid systems to form a UNH crystalline phase and were studied using DR UV-Vis-NIR spectroscopy. We have shown the first, directly observed NpO_2^{2+} solid-state absorbance band at 1089 nm, supporting earlier reports of a potential band in the range of 1080 nm.

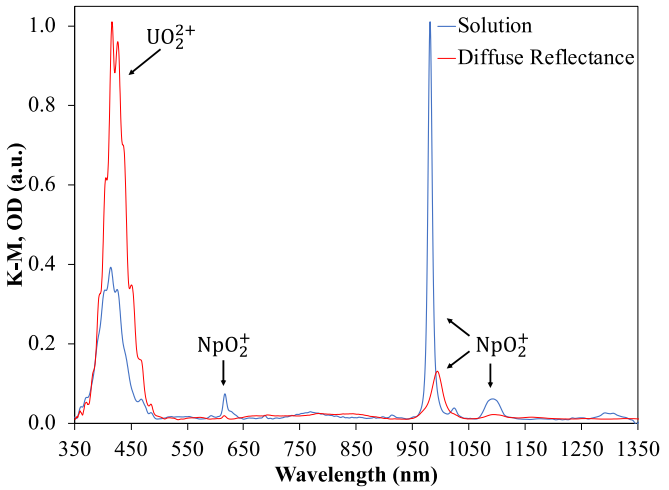

Fig. 6 Absorbance spectra of the NpO_2^+ uranyl nitrate solution prior to crystallization diluted 100-fold (blue) and Kubelka-Munk function of the crystallized UNH with NpO_2^+ incorporated (red) normalized to 1 for comparison.

Moreover, to the best of our knowledge, we have observed the first reported AmO_2^{2+} and NpO_2^+ solid-state absorbance bands at 958 nm and 994 nm, respectively. Upon washing a portion of the AmO_2^{2+} containing crystalline phase, no change was observed in the 958 nm absorbance, indicating the AmO_2^{2+} was present homogenously within the lattice, rather than concentrated near or on the surface. With regards to nuclear fuel recycle, these studies are a first step toward validating the hypothesis that the AnO_2^{2+} TRUs are incorporated into the UNH lattice structure, replacing UO_2^{2+}. Such an approach would open the door to a whole new paradigm of used nuclear fuel recycle, as an attractive single-technology alternative to the systems of multiple solvent-extraction steps that previously have been demonstrated.

Conflicts of interest

There are no conflicts to declare.

Acknowledgements

This work was sponsored by the Nuclear Energy University Program, Office of Nuclear Energy, U.S. Department of Energy, under Award No. DE-NE0008653, for which the authors are very grateful. The transuranic isotopes used in this research were supplied by the United States Department of Energy Office of Science by the Isotope Program in the Office of Nuclear Physics. We want to acknowledge Dr. Luis H. Ortega of the Fuel Cycle and Materials Laboratory in the Department of Nuclear Engineering at Texas A&M University who aided in obtaining the SEM images and EDS measurements.

Notes and references

1 P. A. Kharecha and J. E. Hansen, *Environ. Sci. Technol.*, 2013, **47**, 4889–95.
2 R. W. Grimes and W. J. Nuttall, *Science*, 2010, **329**, 799–803.
3 W. C. Sailor, *Science*, 2000, **288**, 1177–1178.
4 S. Tachimori and Y. Morita, in *Ion Exchange and Solvent Extraction A Series of Advances, Volume 19*, ed. B. A. Moyer, CRC Press, Philadelphia, 2009, pp. 1–63.
5 C. Poinssot, B. Boullis and S. Bourg, in *Reprocessing and Recycling of Spent Nuclear Fuel*, ed. R. Taylor, Elsevier, Cambridge, 2015, pp. 27–48.
6 M. Salvatores and G. Palmiotti, *Prog. Part. Nucl. Phys.*, 2011, **66**, 144–166.
7 R. A. Wigeland, T. H. Bauer, T. H. Fanning and E. E. Morris, *Nucl. Technol.*, 2006, **154**, 95–106.
8 T. A. Todd and R. A. Wigeland, in *Separations for the Nuclear Fuel Cycle in the 21 st Century*, eds. G. J. Lumetta, K. L. Nash, S. B. Clark and J. I. Friese, American Chemical Society, Washington, DC, 2006, vol. 933, pp. 41–55.
9 V. Manchanda, P. Pathak and P. Mohapatra, in *Ion Exchange and Solvent Extraction A Series of Advances, Volume 19*, ed. B. A. Moyer, CRC Press, Philadelphia, 2009, pp. 65–118.
10 S. A. Ansari, P. Pathak, P. K. Mohapatra and V. K. Manchanda, *Sep. Purif. Rev.*, 2011, **40**, 43–76.
11 R. A. Wigeland, T. Taiwo and M. Todosow, in *Global 2015*, Paris, France, 2015, pp. 329–335.
12 M. Miguirditchian, L. Chareyre, X. Heres, C. Hill, P. Baron and M. Masson, in *GLOBAL 2007*, American Nuclear Society, La Grange Park, IL, 2007, pp. 550–552.
13 E. Aneheim, C. Ekberg, A. Fermvik, M. R. S. J. Foreman, T. Retegan and G. Skarnemark, *Solvent Extr. Ion Exch.*, 2010, **28**, 437–458.
14 W. H. Runde and B. J. Mincher, *Chem. Rev.*, 2011, **111**, 5723–5741.
15 B. A. Moyer, G. J. Lumetta and B. J. Mincher, in *Reprocessing and Recycling of Spent Nuclear Fuel*, Elsevier, Cambridge, 2015, pp. 289–312.
16 J. D. Burns and B. A. Moyer, *Inorg. Chem.*, 2016, **55**, 8913–8919.
17 J. D. Burns and B. A. Moyer, *J. Clean. Prod.*, 2018, **172**, 867–871.
18 C. J. Dares, A. M. Lapides, B. J. Mincher and T. J. Meyer, *Science*, 2015, **350**, 652–655.
19 P. Lindqvist-Reis, C. Apostolidis, O. Walter, R. Marsac, N. L. Banik, M. Y. Skripkin, J. Rothe and A. Morgenstern, *Dalt. Trans.*, 2013, **42**, 15275.
20 N. A. Meredith, M. J. Polinski, J. N. Cross, E. M. Villa, A. Simonetti and T. E. Albrecht-Schmitt, *Cryst. Growth Des.*, 2013, **13**, 386–392.
21 A. J. Gaunt, I. May, M. P. Neu, S. D. Reilly and B. L. Scott, *Inorg. Chem.*, 2011, **50**, 4244–4246.
22 P. R. Zalupski, T. S. Grimes, C. R. Heathman and D. R. Peterman, *Appl. Spectrosc.*, 2017, **71**, 2608–2615.

$$(1-x)UO_2^{2+} + xAnO_2^{2+} + 2NO_3^- + 6H_2O \rightarrow (UO_2)_{1-x}(AnO_2)_x(NO_3)_2 \cdot 6H_2O$$